OPEN

Citation: Cell Death and Disease (2014) 5, e1423; doi:10.1038/cddis.2014.365

www.nature.com/cddis

Radiosensitization by a novel Bcl-2 and Bcl-X_L inhibitor S44563 in small-cell lung cancer

Y Loriot[1,2,3], P Mordant[1,2,3], D Dugue[1,2], O Geneste[4], A Gombos[1,2], P Opolon[1,2], J Guegan[5], J-L Perfettini[1,2,3], A Pierre[4], LK Berthier[4], G Kroemer[6,7,8,9], JC Soria[1,3,10], S Depil[4] and E Deutsch*[,1,2,3]

Radiotherapy has a critical role in the treatment of small-cell lung cancer (SCLC). The effectiveness of radiation in SCLC remains limited as resistance results from defects in apoptosis. In the current study, we investigated whether using the Bcl-2/Bcl-X_L inhibitor S44563 can enhance radiosensitivity of SCLC cells *in vitro* and *in vivo*. *In vitro* studies confirmed that S44563 caused SCLC cells to acquire hallmarks of apoptosis. S44563 markedly enhanced the sensitivity of SCLC cells to radiation, as determined by a clonogenic assay. The combination of S44563 and cisplatin-based chemo-radiation showed a significant tumor growth delay and increased overall survival in mouse xenograft models. This positive interaction was greater when S44563 was given after the completion of the radiation, which might be explained by the radiation-induced overexpression of anti-apoptotic proteins secondary to activation of the NF-κB pathway. These data underline the possibility of combining IR and Bcl-2/Bcl-X_L inhibition in the treatment of SCLC as they underscore the importance of administering conventional and targeted therapies in an optimal sequence.

Cell Death and Disease (2014) **5,** e1423; doi:10.1038/cddis.2014.365; published online 18 September 2014

Identifying the mechanisms leading to radioresistance including resistance to apoptosis is essential to improve clinical outcome in cancer patients. Disabled apoptosis has been catalogued among the fundamental hallmarks of cancer[1] and the proteins of the Bcl-2 family play a fundamental role in regulating this modality of cell death. The Bcl-2 family comprises both pro- and anti-apoptotic members; the latter (Bcl-2, Bcl-X_L and Mcl-1) are often overexpressed in cancer cells to facilitate the survival of cells that under normal circumstances should have undergone apoptosis.[2] The molecular interactions between pro- and anti-apoptotic Bcl-2 family members determine cellular sensitivity to multiple lethal triggers, including many standard chemotherapeutic agents and ionizing radiation (IR).[3,4] Overexpression of Bcl-2 is known to increase clonogenic survival and inhibit IR-induced apoptosis.[3,4] Bcl-X_L expression also shows a strong correlation with resistance to cytotoxic anticancer therapies including IR.[5,6]

Lung cancer is the leading cause of cancer deaths in western countries.[7] Small-cell lung cancer (SCLC) accounts for 15% of all lung cancer cases and is distinguished from non-SCLC by its characteristic cytomorphology, rapid proliferation and early dissemination to metastatic sites.[8] The standard of care to patients with limited-stage SCLC and good performance status is based on a combination of IR and cisplatin-based chemotherapy, resulting in a complete response rate as high as 50–80% coupled to a deceptive 12–20% 5-year survival.[9] Initially, SCLC is responsive to chemo- and radiotherapy. However, SCLC recurs within the first 12 months.[10] To date, the pathways mediating chemo- and radioresistance in SCLC are largely unknown.

Deletion of pro-apoptotic gene and amplification of anti-apoptotic gene are frequently observed in SCLC, especially amplification of the *BCL2L1* and *BCL2L2* genes.[11] At the protein level, increased expression of Bcl-2 has been reported in up to 90% of metastatic SCLC. Bcl-2 overexpression, downregulation of the pro-apoptotic Bcl-2 antagonist Bax and a shift in the Bcl-2/Bax ratio to levels >1 are correlated with lower apoptotic index in tumors[12] and are associated with chemotherapeutic resistance in SCLC cell lines.[13] In contrast with most solid tumor cell lines, where apoptosis does not appear as a predominant cell death mechanism after IR,[14] overexpression of Bcl-2 can abrogate chemotherapy-induced apoptosis in SCLC cell lines.[13] Apoptosis may be one of the mechanisms that cause SCLC cells to die in response to radiotherapy.[15,16]

Recently, a small synthetic compound ABT-737 and its orally bioavailable form ABT-263 (Navitoclax) were shown to efficiently antagonize Bcl-2 and Bcl-X_L by binding to their BH3 receptor domain. ABT737 or its derivatives mediate anti-tumoral effects in chronic lymphocytic leukemia (CLL) and

[1]Gustave Roussy, Cancer Campus, Grand Paris, 114 rue Edouard Vaillant, Villejuif 94805, France; [2]INSERM 1030 "radiosensitivity and human carcinogenesis", 114 rue Edouard Vaillant, Villejuif 94805, France; [3]Faculty of Medicine, University of Paris-Sud, DHU TORINO, LABEX LERMIT, SIRIC Socrates, Le Kremlin-Bicêtre, France; [4]Institut de Recherche Servier Oncology R&D Unit, 125 Chemin De Ronde, Croissy Sur Seine 78290, France; [5]Institut Gustave Roussy's Genomics Centre, Institut de cancérologie Gustave-Roussy, 114, rue Edouard-Vaillant, Villejuif 94805, France; [6]INSERM, U848, Villejuif, France; [7]Metabolomics Platform, Institut Gustave Roussy, Villejuif, France; [8]Centre de Recherche des Cordeliers, Paris, France; [9]Pôle de Biologie, Hôpital Européen Georges Pompidou, AP-HP, Paris, France and [10]Inserm 981, Institut de cancérologie Gustave-Roussy, 114, rue Edouard-Vaillant, Villejuif 94805, France

*Corresponding author: E Deutsch, Inserm 1030 "Radiosensitivity and human radiocarcinogenesis", Institut de cancérologie Gustave-Roussy, 114, rue Edouard-Vaillant, Villejuif 94805, France. Tel: +33 (0)1 42 11 65 73; Fax: +33 1 42 11 52 99; E-mail: deutsch@igr.fr

Abbreviations: BLM, bleomycin; DER, dose enhancement ratio; FP, fluorescence polarization; GAPDH, glyceraldehyde-3-phosphate dehydrogenase; IC50, half-inhibitory concentration; IR, ionizing radiation; NPM, nucleoplasmin; RTV, relative tumor volume; SCLC, small cell lung cancer; silencing RNA, siRNA; SF, surviving fraction

Received 31.3.14; revised 06.6.14; accepted 26.6.14; Edited by G Melino

SCLC in preclinical and early clinical trials.[17,18] However, there is no published study that evaluates the combination of new Bcl-2/Bcl-X_L inhibitors, IR and chemo-radiotherapy.

Results

Anti-apoptotic proteins are frequently expressed in localized SCLC specimens. To investigate the frequency of anti-apoptotic proteins in SCLC, we first assessed whether anti-apoptotic proteins such as Bcl-2, Bcl-X_L and Mcl-1 were overexpressed in a tissue microarray including 29 localized SCLC that had been surgically removed (Supplementary Figure 1). Bcl-2, Bcl-X_L and Mcl-1 were expressed at high levels in 17 (60%), 24 (85%) and 20 specimens (70%). To assess whether overexpression of these proteins might be related to gene amplification, we extracted *in silico* microarray data from a public database including 40 SCLC samples and 23 cell lines.[19] In this study, no copy number alteration was found for *BCL2* and *BCL-XL* gene. By contrast, *MCL1* gene amplification was observed in 57% of samples. In contrast, none of the SCLC tumors or cell lines exhibited copy number alteration for *BCL2* and *BCL-XL* gene (Supplementary Figure 2). We also assessed the expression of various pro- and anti-apoptotic proteins in the three SCLC cell lines that we used in preclinical experiments (Supplementary Figure 1), confirming the expression of Bcl-X_L in all cell lines, that of Mcl-1 in H196 (but not H69 and H146), and that of Bcl-2 in H69 and H146 (but not in H196). Expression of various pro- and anti-apoptotic proteins in the three SCLC cell lines were also consistent with a previous report.[20]

S44563 is a potent binder of Bcl-2 and Bcl-X_L. We determined the capacity of a new BH3 peptide mimetic, S44563 (Figure 1a), to displace a fluorescent Puma BH3 peptide from recombinant Bcl-2 or Bcl-X_L by fluorescence polarization (FP) assays, using recombinant Bcl-2 or Bcl- X_L and a fluorescent Puma BH3 peptide. Figure 1b shows the inhibition of Bcl-2 and Bcl- X_L, respectively, by S44563 demonstrating that S44563 is a potent binder of Bcl-2 and Bcl-X_L. The half-inhibitory concentration (IC_{50}) of S44563 required to inhibit them in a Bcl-2/F-Puma BH3 interaction assay and the Bcl-X_L/F-Puma BH3 interaction were measured as 131 nM (95% CI:123–139 nM) and 140 nM (130–150 nM), respectively.

S44563 potently induces apoptosis in Bcl-2 overexpressing SCLC cells. The H146 SCLC cell line is known to overexpress Bcl-2 because of a gene amplification and depends in its survival on Bcl-2.[21,22] To evaluate Bcl-2 target hitting in a cell-based experiment, Bcl-2/Bax co-immunoprecipitation assays were performed from lysates of H146 cells that were left untreated or were treated with S44563 for 2 h. As shown in Figure 1c, S44563 efficiently disrupted the Bcl-2/Bax interaction in H146 cells in a dose-dependent manner that was compatible with its *in vitro* effects on Bcl-2 and Bcl-X_L. The effect of S44563 on this interaction is clearly visible at 0.1 μM and is more pronounced at 1 μM. Upon prolonged treatment (6 h), H146 cells exposed to S44563 exhibited a significant increase in a caspase-3-like enzymatic activity capable of cleaving a synthetic substrate containing the peptide motif DEVD (Figure 1d). The rapid kinetics of induction of this is a strong inducer of DEVDase activity and is consistent with the mechanism of action of S44563, which directly releases the apoptotic machinery from inhibition by anti-apoptotic proteins (Bcl-2 and Bcl- X_L). The capacity of S44563 to reduce the viability of H146 cells was measured by means of the cell proliferation assay, revealing an IC_{50} of 311 nM (238–407). Side-to-side comparison showed that S44563 and ABT-263 in several cancer cell lines including H146 cell line did not show any difference for efficacy and toxicity in a cell viability assay (Supplementary Table 1). These data demonstrate that S44563 potently triggers apoptosis in Bcl-2-dependent H146 cells.

S44563 has a differential effect on three distinct SCLC cell lines. To examine the sensitivity of SCLC cell lines to S44563, we assessed the impact of S44563 on cell viability by means of a cell proliferation assay (Figure 1e) and a clonogenic survival assay (Supplementary Figure 3). S44563 was particularly effective on Bcl-2-overexpressing H146 cells, less so on H69 cells and had no major effect on Mcl-1-expressing H196 cells, which resisted micromolar concentrations of S44563. Addition of the caspase inhibitor Z-VAD-FMK strongly reduced the negative effect of S44563 on the viability of H146 cells (Supplementary Figure 4).

To determine whether the effect on cell survival was mediated by apoptosis induction, we assessed the generation of cleaved caspase-3 and the dissipation of the mitochondrial inner transmembrane potential. Whereas the sensitive cell line (H146) accumulated proteolytically mature caspase- 3, the resistant cell line (H196) did not manifest such an effect (Figure 2a). H146 cells cultured with S44563 manifested a dose- and time-dependent dissipation of the mitochondrial inner transmembrane potential ($\Delta\Psi_m$, as assessed by staining with the $\Delta\Psi_m$ potential-sensitive probe $DiOC_6(10)$) and the permeabilization of the plasma membrane (as measured by staining with the vital dye propidium iodide) (Figure 2b). These results suggest that monotherapy with S44563 induces apoptosis (rather than other cell death modalities) in H146 cells.

S44563 induces the mitochondrial caspase activation pathway. To investigate the cellular effects of S44563, we assessed the effects of S44563 on mitochondrial pathways using immunoblot and cytometry analysis. We showed that the lethal effect of S44563 is mediated through induction and activation of mitochondrial apoptosis pathway. Thus, H146 cells treated with S44563 manifested caspase-3 activation, as determined by immunoblotting (Figure 2c). S44563 activated caspases that contribute to the mitochondrial pathway, including caspase-9 and caspase-3 (Figure 2c), yet failed to induce the proteolytic maturation of caspase-8, which characterizes the extrinsic pathway of apoptosis. Blockade of caspase activation by the broad-spectrum inhibitor Z-VAD-FMK delayed cell death induced by S44563 and blocked the accumulation of cells with a hypoploid (sub G1) DNA content induced by S44563 (Figure 2d). In another model using *BAX* knockout HCT116 cells, we did not find any

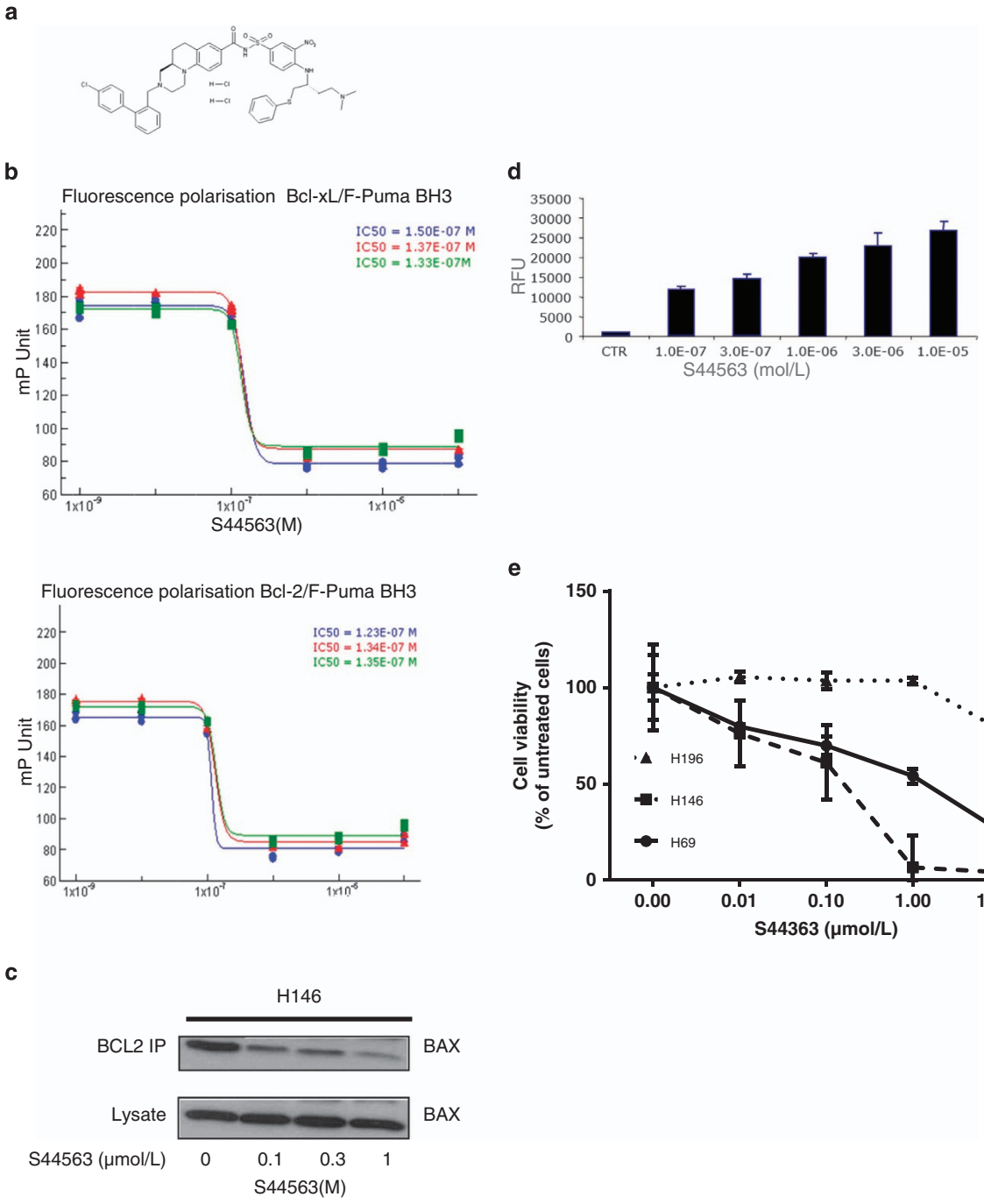

Figure 1 Effect of S44563 on cell viability and cell survival. (**a**) Chemical structure of S44563. (**b**) Inhibition of the interaction between Bcl-2 or Bcl-X_L and fluorescent Puma BH3 peptide measured by the decrease of fluorescence polarization as a function of S44563 concentrations. Three independent experiments are presented. FP data are presented in millipolarization units (mP). Each experiment was performed in triplicates (mean +/− S.E.M., three experiments). (**c**) Bcl-2/Bax complex disruption by S44563 measured by co-immunoprecipitation assays. Cell lysates were subjected to immunoprecipitation with an anti-Bcl-2 antibody and immunoprecipitates and lysates were analyzed by immunoblot with an anti-Bax antibody. (**d**) Caspase 3 activation by S44563 in H146 cell line. Caspase 3 enzymatic activity is presented as Relative Fluorescent Unit (RFU) per minute and per mg of protein (mean +/− S.E.M., three experiments). (**e**) Inhibition of SCLC cell proliferation by S44563. The cells were seeded 24 h before S44563 was administered with various concentrations from 10 nmol/l to 10 μmol/l for 72 h. The number of viable cells was determined by using WST-1 assay according to the manufactrurer's instructions (Roche). Absorbance values were normalized to the values obtained from untreated cells to determine survival rates. Each assay was performed in triplicate (points, mean; bars, standard error deviation, three experiments)

cytochrome c in the cytosol sub-fraction whereas in *BAX* wild-type HCT116 cells, cytochrome c was released from mitochondria with a dose-dependent manner indicating that S44563 induces the release of cytochrome c from mitochondria (Supplementary Figure 5). Consistent with the *in vitro* activity of S44563 against SCLC cells, S44563 showed a

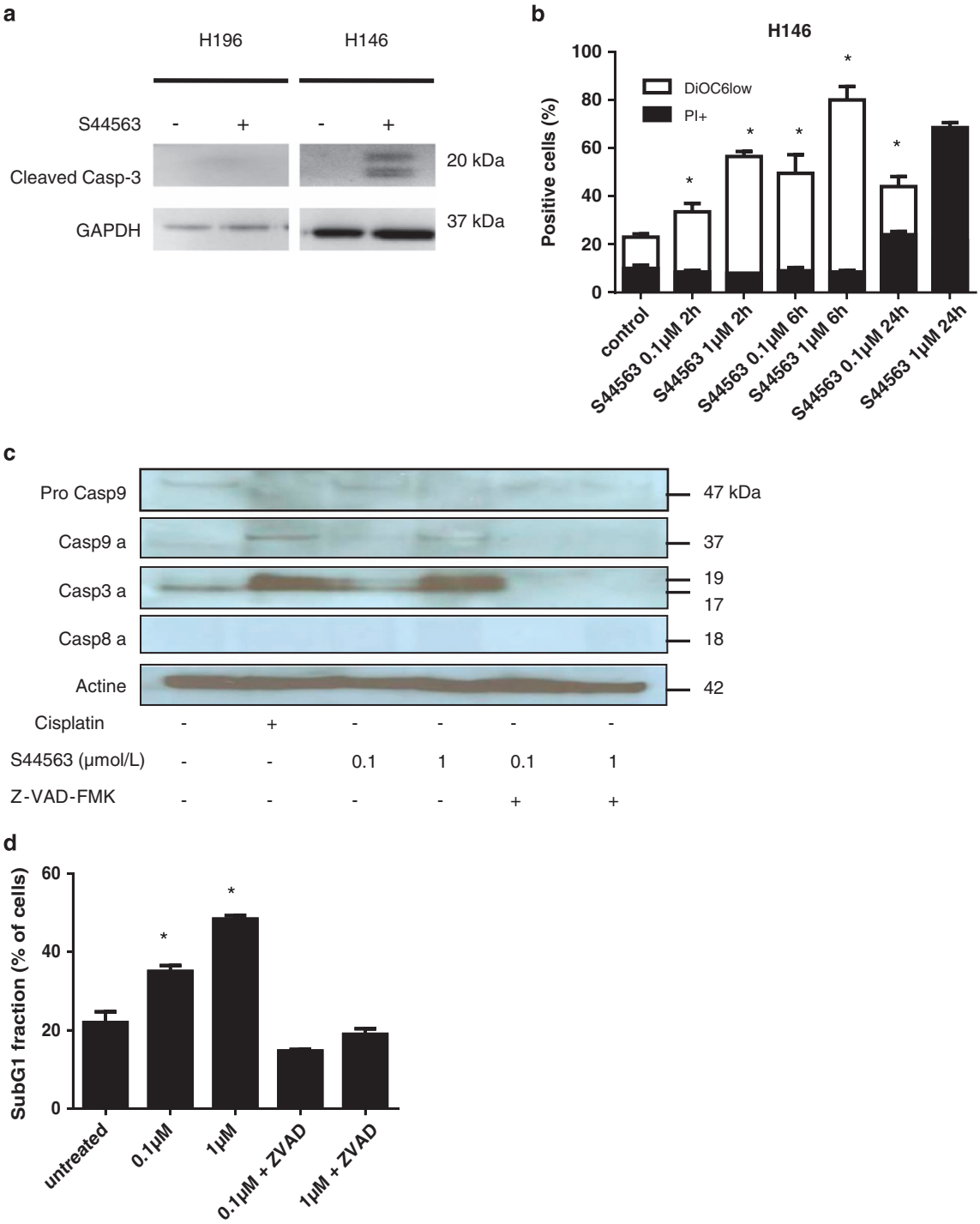

Figure 2 The effect of S44563 on apoptosis activation. (**a**) Distinct apoptotic response to S44563 in SCLC cells lines. SCLC cells were incubated with S44563 at a dose of 100 nmol/l for 24 h and then were harvested for immunoblotting. The monoclonal mouse anti-human cleaved caspase 3 clone 100 (1 : 500 dilution; Cell signaling), was used. (**b**) Effect of S44563 on the dissipation of the mitochondrial transmembrane potential. H146 cells were harvested after different time exposure to S44563 at different concentrations. Cells were then washed with PBS and stained with the following probes to assess apoptosis-associated modifications: propidium iodide (2 μg/ml, Sigma-Aldrich) for viability and dihexyloxacarbocyanine iodide ($DiOC_6(3)$, 40 nmol/l, Molecular Probes) for $\Delta\psi_m$ dissipation (columns, mean: bars, standard error deviation; $^*P < 0.05$ for DiOC6low fractions as compared with control). Experiments were performed in triplicate. Results from two experiments were pooled. (**c**) Effect of S44563 on caspase activation. H146 cells were incubated with S44563 at different doses of S44563 with or without (Z-VAD-FMK, 20 μmol/l) for 24 h and then were harvested for immunoblotting. The monoclonal mouse anti-human cleaved caspase-3 clone 100 (1 : 500 dilution; Cell signaling), cleaved and full-length caspase-9 (1 : 500 dilution, Cell signaling), and cleaved caspase- 8 (1 : 500 dilution; Cell signaling) were used. (**d**) Effect of S44563 on sub-G1 phase induction. Cells were harvested after 24 h exposure to S44563 at different concentrations with or without the pan-caspase inhibitor *N*-benzyloxycarbonyl-Val-Ala-Asp-fluoromethylketone (Z-VAD-FMK, 20 μmol/l, from Bachem, Weil am Rhein, Germany). Resulting DNA distributions were analyzed by Modfit (Verity Software House, Inc., Topsham, ME, USA) for the proportion of cells in sub-G_0, G_1, and G_2-M phases of the cell cycle (columns, mean; bars, standard deviation). Experiments were performed in triplicate. Results from two experiments were combined

significant antitumor activity when administered intraperitoneally once a day for 21 days in a H146 xenograft model. This tumor regression lasted for more than 50 days after the end of treatment (Supplementary Figure 6a). No weight loss was observed over the time course of the experiment (Supplementary Figure 6b), suggesting that S44563 can mediate anticancer effects at an acceptable level of toxicity.

S44563 sensitizes SCLC cell lines to radiation. To determine the radiosensitivity of SCLC cells, we performed a clonogenic survival assay using IR at different doses. SCLC cells exhibited different sensitivity to radiation. Surviving fraction at 2 Gy (SF2) values ranges from 0.35 to 0.86 (data not shown). In this assay, 100 nmol/l of S44563 radiosensitized H69 and H146 cells, yet had no effect on H196 cells. For this latter cell line, a 100 times higher concentration of S44563 (10 μM) was required to mediate radiosensitization (Figure 3a).

Radiosensitization by S44563 was associated with an increase in sub-G1 fraction and caspase-3 activation. To determine the mechanisms of S44563-mediated radiosensitization, we performed cell cycle profiling of H146 and H196 cells treated with S44563 or radiation, alone or in combination. In S44563-sensitive cells (H146 cells), the combination of radiation and S44563 significantly enhanced radiation-induced apoptosis at 72 h (Figure 3b, $P<0.05$). Conversely, in the resistant H196 cells, the combination of S44563 and radiation induced the induction of apoptosis at 72 h only at a dose of 10 μmol/l of S44563 (data not shown). In both cell lines, S44563 had a minimal effect on the radiation-induced G2/M arrest. The combination of IR and low concentration of S44563 (100 nmol/l) also was more efficient in inducing the proteolytic maturation of caspase-3 expression than the monotherapies in H146 cells (Figure 3c). Taken together, these results suggest that S44563-mediated radiosensitization may be mediated by enhanced apoptosis.

The combination of radiation and S44563 results in better survival in SCLC xenografts. Both H146 and H69 cells that were xenotransplanted into immunodeficient mice developed tumor that could be treated particularly efficiently by the combination of S44563 and IR, as determined by mouse survival in Kaplan–Meier curves (Figure 4a, Supplementary Table 2). In the H146 and H69 xenograft models, there was a significant antitumor effect in the mice treated with radiation (Figure 4b). S44563 plus radiation induced more apoptosis than either S44563 or radiation alone, as determined by immunohistochemical detection of active caspase-3 on H146 tumors excised 24 h after the last treatment (Figure 4c). All treatments appeared to be well tolerated, with no evidence of treatment-related weight loss (data not shown). Moreover, we did not observe any S44563-mediated increase in radiation-induced endothelial damage and fibrosis-like lesions (21) suggesting that the combination of radiation and S44563 is safe (Supplementary Figure 7).

S44563 plus chemoradiotherapy prolongs survival in mice bearing H146 xenografts. Because the standard of care of localized SCLC is radiochemotherapy, that is, the association of IR and cisplatin-based chemotherapy, we assessed the potential value of adding S44563 to chemo-radiotherapy. The triple combination resulted in more frequent complete response of H146 xenografts and decreased median tumor growth, as compared with IR alone and all other groups including S44563 alone or IR + cisplatin alone (Supplementary Table 3). Median tumor volume were analyzed using two-way analysis (ANOVA: Treatment and Time) of variance with repeated measures on factor Time (*post hoc* analysis of Treatment effect at fixed Time levels with Dunnett test). The triple combination induced significant reduction of tumor volumes as compared with other therapies (Supplementary Table 3). Kaplan–Meier survival plots confirmed that the triple combination was more efficient than any of its components alone or in dual combinations (Figure 5a). Similar results were obtained on H69 xenografts, although no complete responses were obtained (Figure 5b, Supplementary Table 3).

Radiation increased anti-apoptotic proteins expression. To investigate the effects of radiation on anti-apoptotic proteins expression, we irradiated xenograft-bearing mice at baseline, as well as when the tumors recurred after the first round of radiotherapy (Supplementary Figure 8). We observed an upregulation of some anti-apoptotic proteins mainly with Bcl-X_L in both situations following fractionated radiation. These data were consistent in different independent experiments with the different cell lines (H146 and H69) (Figure 6a). As we detected an increased expression of anti-apoptotic proteins following fractionated radiation, we hypothesized that S44563 after (rather than concomitant with) tumor irradiation would be particularly efficient because the BH3 mimetic would target Bcl-X_L when the levels of this protein is particularly high.

To test this hypothesis, mice bearing H69 xenografts were treated as above (with concomitant IR and S44563) or sequentially, when S44563 was administered only during the 5 days following the completion of radiotherapy. On day 49, mean tumor volume was significantly reduced in the sequential group (465 mm^3) as compared with the concomitant group (704 mm^3) and radiation alone (1261 mm^3) ($P=0.04$, two-way ANOVA test) (Figure 6b).

To characterize the mechanisms through which S44563 induces radiosensitization, we determined its transcriptional effects at 24 h, as measured at the concentration of S44563 that would kill 50% of the cells at 48 h (100 nmol/l for H146 and 1 μmol/l for H69 cells) by microarray experiments. At 24 h, S44563 did not cause any consistent upregulation or the downregulation of genes involved in DNA reparation or checkpoint control (data not shown). However, when tumor cells were treated with radiation alone, we observed an upregulation of genes, such as *RELB, NF-κB1* and *LTB*, of NF-κB pathway known for being involved in resistance to apoptosis (Supplementary Table 4) qPCR assays confirmed that several genes belonging to NF-κB pathway are upregulated in SCLC cell lines at an early time (Figure 6c), especially *TNF* and *LTB*, which may promote the nuclear translocation of *RELA (p65)*.[23,24] Indeed, RelA/p65 could be detected in the nuclei from the nuclei of H146 cells following radiation of SCLC (Figure 6d), concomitant with the upregulation of Bcl-X_L

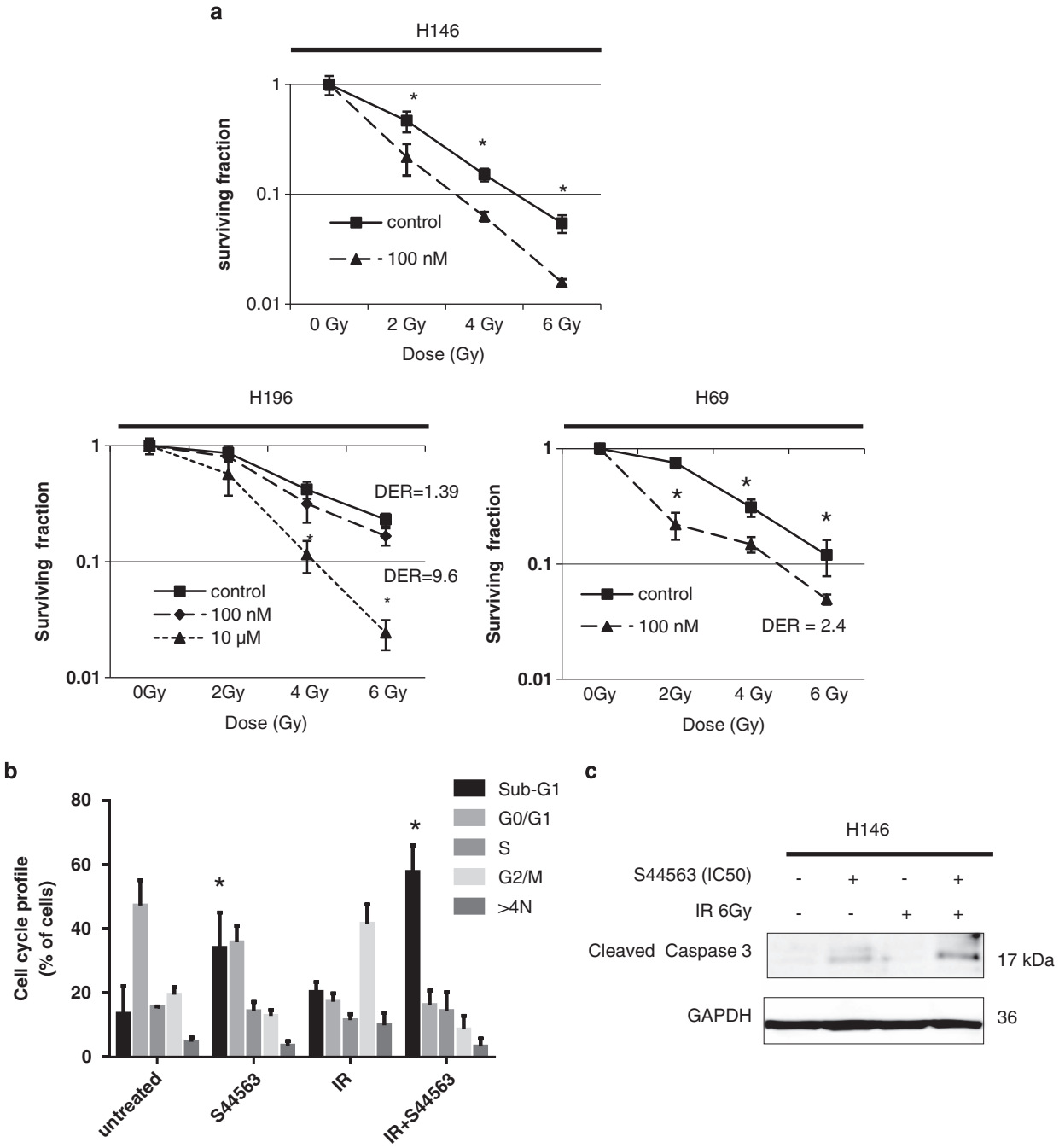

Figure 3 The effects of S44563 on tumor cell radiosensitivity. (**a**) Effect of S44563 on SCLC cells radiosensitivity. The SCLC cells were seeded for colony formation in 35 mm dishes containing methylcellulose-based medium at 500–10 000 cells/dish with various doses of S44563 for 21–28 days period. Radiation was given 2 h after incubating cells in methylcellulose-based medium containing S44563. Upon intervals of 21–28 days, colonies were manually counted using microscopy. All colonies of 50 cells or more were then counted. The survival fraction (SF) was estimated according to the formula: SF = number of colonies formed/number of cells seeded plating efficiency of the control group. Experiments were performed in triplicate (points, mean; bars, standard deviation, $*P < 0.05$ as compared with unirradiated cells). The figure is representative of four independent experiments. (**b**) Effect of S44563 on radiation-induced sub-G1 fraction. Radiation was given at a dose of 6 Gy 2 h after giving S44563 at a dose of 100 nmol/l for H146 cells. Cells were harvested after 72 h exposure to S44563 and stained with a propidium iodide solution for 24 h. Stained nuclei were analyzed for DNA-propidium iodide fluorescence using a Becton Dickinson FACScan flow cytometer. Resulting DNA distributions were analyzed by Modfit (Verity Software House, Inc.) for the proportion of cells in sub-G_0, G_1, and G_2-M phases of the cell cycle (columns, mean; bars, standard deviation, $*P < 0.05$ as compared with untreated cells). Results from two experiments were combined. (**c**) The H146 cells were treated as experiment 3B and immunoblotting for cleaved caspase 3 was performed. The ratio of cleaved caspase 3/GAPDH was measured using dedicated software. The combination of radiation and S44563 results in 2.5-fold enhancement of cleaved caspase 3/GAPDH ratio

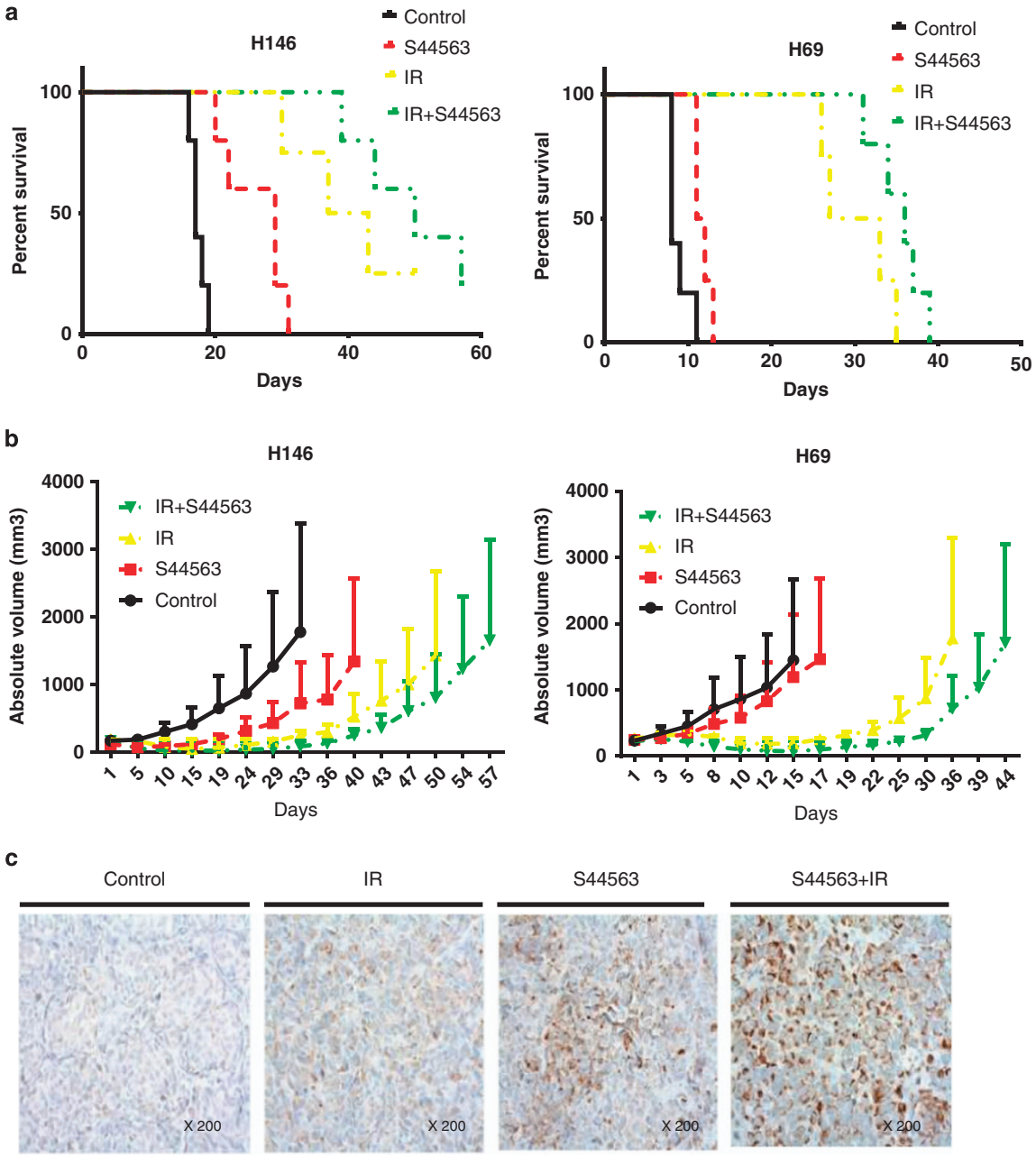

Figure 4 S44563 enhanced the efficacy of radiotherapy in SCLC xenograft tumors and prolonged overall survival. (**a**) H146 (left part) and H69 xenograft tumor (right part). Kaplan–Meier survival curves after treatment with fractionated X-ray irradiation and S44563, alone or in combination. When tumors reached the appropriate size, the mice were randomized into 5–10 mice per group and treated with either S44563 100 mg/kg i.p., × 5 days or X-ray irradiation 2 Gy × 4, × 1 week, or their combination. The pictures are representative of two experiments. For each experiment, 6–10 mice were used for each group. Kaplan–Meier survival curves reflect significantly enhanced antitumor efficacy using IR + S44563 regimen. The endpoint was relative tumor volume triple the initial tumor volume (RTV3). Log-rank test analysis demonstrated that the combination resulted in improved survival compared with S44563 or radiation alone ($P = 0.1$ in H146 xenografts; $P < 0.05$ in H69 xenografts). (**b**) Tumor growth volumes curves. Volume growth was analyzed on day 50 for H146 ($P = 0.1$) and on day 37 for H69 xenografts ($P = 0.1$). Standard deviations are shown. (**c**) H146-bearing mice were treated with S44563 (100 mg/kg, d1–d5), IR (four fractions, 2 Gy per fraction) or both and then were killed 2 h after the last treatment. Tumors were excised and stained for cleaved caspase-3

(Figure 6e). Silencing p65 prevented radiation-induced expression of Bcl-2 in H146 cells and Bcl-X_L in H196 cells (Figure 6f).

Taken together, these data suggest that S44563 might be advantageously employed as a radiosensitizing agent, especially when it is used during the IR-induced increase in the expression of its targets, Bcl-2 and Bcl-X_L.

Discussion

The data contained in this work outline a strategy for the treatment of SCLC, based on concomitant and adjuvant administration of a novel Bcl-2 and Bcl-X_L inhibitor, S44563 with IR. This strategy of radiosensitization (to improve the outcome of radiotherapy) or radiochemosensitization

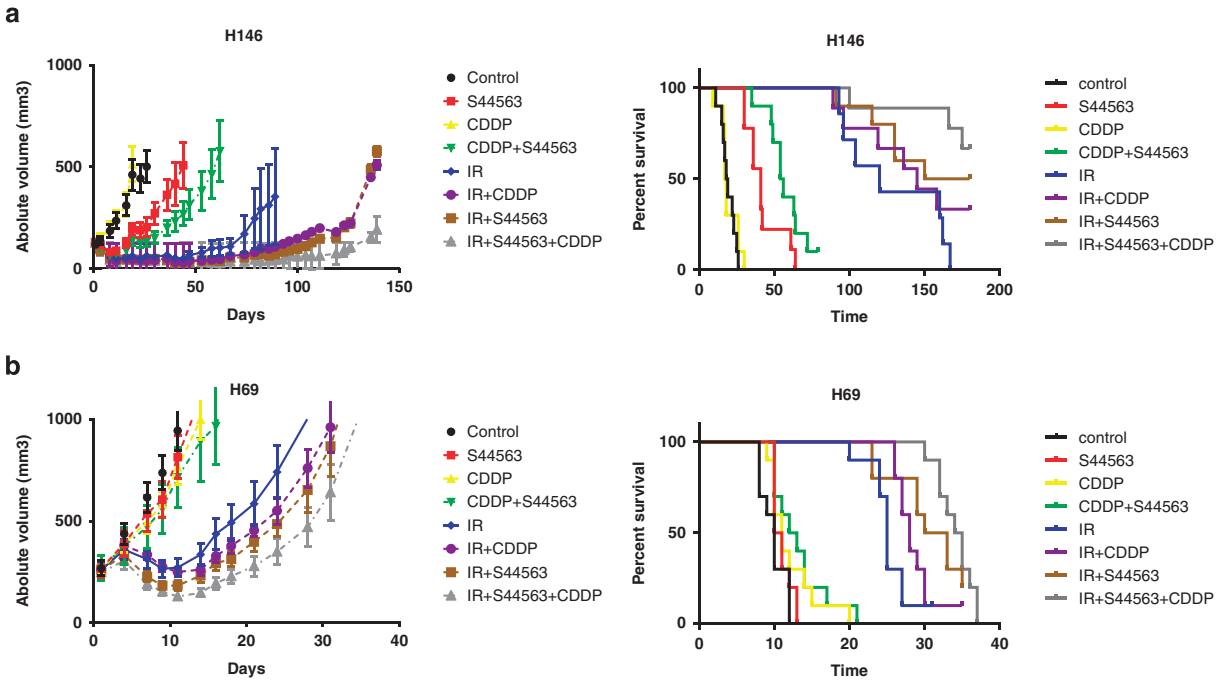

Figure 5 S44563 enhanced the efficacy of cisplatin-based chemo-radiotherapy in SCLC xenograft tumors. H146 (**a**) and H69 xenograft tumor (**b**) Kaplan–Meier and tumor growth volume curves after treatment with fractionated X-ray irradiation and S44563, cisplatin alone or in combination. When tumors reached the appropriate size, the mice were randomized into 10 mice per group and treated with either S44563 100 mg/kg i.p., × 5 days or X-ray irradiation 2 Gy × 4, × 1 week, cisplatin 1 mg/kg daily given twice per week for 2 weeks or their combination

(to improve the outcome of radiotherapy combined with cisplatin-based chemotherapy) may be particularly efficient when S44563 is applied to cancers that exhibit high levels of Bcl-2 of Bcl-X_L. Indeed, there is a molecular heterogeneity among SCLC in thus far that some tumors depend on Bcl-2 of Bcl-X_L (and hence can be expected to respond to S44563) and others depend on Mcl-1 (and hence must be refractory to S44563). Moreover, Bcl-2 of Bcl-X_L apparently constitute 'moving targets' in the sense that radiotherapy can induce the expression of these proteins, meaning that S44563 is particularly efficient when administered after (rather than during) radiotherapy. This interaction resulted from chemosensitization through the inhibition of radiation-induced Bcl-2 and Bcl-X_L upregulation. The IR-induced upregulation of anti-apoptotic proteins might be mediated through a signal transduction pathway involving NF-κB activation. Activation of NF-κB components such as RELA or RELB by DNA damage has been shown to be involved in resistance to radiotherapy in many cancers.

Many reports have shown that resistance of SCLC to standard treatment may be related to decreased apoptotic response in a subset of SCLC cells. We found that in a collection of localized SCLC removed surgically, anti-apoptotic proteins such as Bcl-2, Bcl-X_L and Mcl-1 were frequently upregulated. Overexpression of Bcl-2 and Bcl-X_L are not fully explained by common gene alterations in SCLC. *BCL2L1* and *BCL2L2* gene amplifications have been reported in previous studies,[11] although others showed that low-level gains of the *BCL2* gene are present in 40% of cases in an array including 62 SCLC samples and high-level gains are observed in only 8% of the tumors.[22] These results are consistent with publicly accessible data banks revealing *MCL1* gene amplification in 57% of samples but no copy number alteration for the genes encoding *BCL2* and *BCL2L1*. Thus, Bcl-2 and Bcl-X_L overexpression could result from alternative mechanisms such as activation of their promoters by transcriptional factors. Furthermore, chemotherapy induces Bcl-2 and Bcl-X_L expression, perhaps explaining in part the acquisition of resistance to cisplatin-based regimens. Here, we showed that radiation itself resulted in the enhanced expression of Bcl-X_L at the mRNA and protein levels, both *in vitro* and *in vivo* through transcriptional event. Intriguingly, several mRNA species involved in the NF-κB pathway were activated following radiation, coupled to enhanced expression of anti-apoptotic proteins expression. Previous studies reported that NF-κB activation by DNA damage played a critical role in the response to radiation through the regulation of anti-apoptotic genes and cell survival induction.[23,24] These data are consistent with a recent study investigating a specific Bcl-X_L inhibitor BXI-72 in NSCLC.[25] In this study, increased levels of Bcl-X_L and Bcl2 were observed in A549-IRR cells as compared with A549 parental cells providing evidence that IR-enhanced Bcl-X_L contributes to acquired radioresistance. BXI-72 repressed tumors derived from both A549-P and A549-IRR cells, indicating that BXI-72 can overcome acquired radioresistance *in vivo*. The majority of the candidate proteins upregulated following radiation were proteins such as, TNF, LTB and NFKB1, that are either expressed in response to stimulation by pro-inflammatory

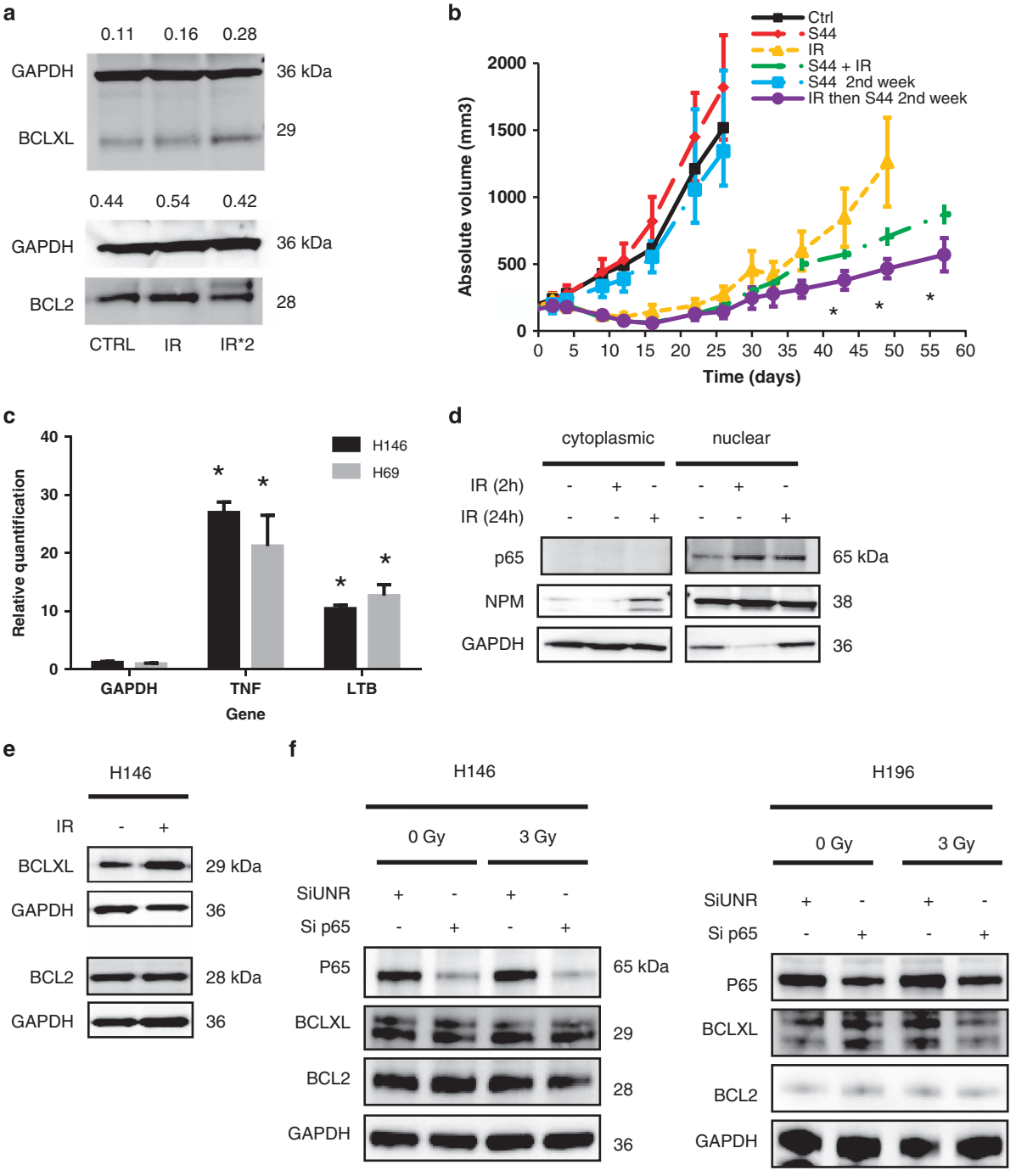

Figure 6 Radiation induced the expression of anti-apoptotic proteins and sensitized SCLC to S44563. (**a**) H69 xenografts were given 3 Gy radiation from day 1 to day 4 (IR), twice (IR*2) when tumors recurred upon the first course of radiation and then were excised when the tumors recurred again. Protein lysates were obtained and blots were stripped with excised for Bcl-2 and Bcl-X_L antibodies expression analysis. Protein/GAPDH ratio (from 0 to 1) were quantified and reported at the top of each lane. (**b**) H69 xenograft tumor curves after treatment with fractionated X-ray irradiation and S44563, alone or in concomitant and sequential combination. When tumors reached appropriate size, the mice were randomized into 5–10 mice per group and treated with either S44563 100 mg/kg i.p., × 5 days or X-ray irradiation 2 Gy × 4, × 1 week, or their combination as in Figure 5. A group in which mice were received S44563 only within the 5 days of the completion of radiotherapy was added. Standard errors are shown (columns, mean; bars, standard error deviation; *$P<0.05$, permutational *t*-tests two-way ANOVA test). (**c**) TNF and LTB gene expression induction following radiation in H16 and H69 cells using real-time PCR. H146 and H69 cells were treated with 2 Gy radiation and harvested either 2 or 24 h after the treatment (columns, mean; bars, standard error deviation; *$P<0.05$ as compared to GAPDH level). Each experiment has been carried out in triplicate. The pictures are representative of three experiments. (**d**) Accumulation of p65/RelA in cell nuclei after irradiation. Nuclear extracts from H146 cells were immunoblotted with specific antibodies to show p65/RelA. Blots were stripped and reprobed with mouse monoclonal anti-nucleoplasmin (NPM) as a control protein loading. Unirradiated cells served as a control. Data from three experiments were combined. (**e**) H146 cells were given one 3-Gy fraction and were then harvested 24 h later for Bcl-2 and, Bcl-X_L immunoblotting. GAPDH was used as the loading control. (**f**) H146 cells and H196 cells were transfected with silencing RNA (siRNA) against p65/RelA (Santa Cruz, sc-29410, final concentration: 15 nmol/l) using Amaxa *Nucleofector* Technology for 24 h and then were irradiated at a dose of 6 Gy. Total lysates were obtained 24 h after irradiation and blots were stripped with p65/RelA, Bcl2 and Bcl-Xl proteins. GAPDH were used as loading control

cytokines or are involved in inflammatory networks.[24,26] These data are consistent with recent reports demonstrating that pro-inflammatory cytokines and inflammatory response pathways play an important role in radioresistance.[26–28] RELA (NF-κB p65) has been shown to promote the expression of *BCLX*$_L$[23,24] as well as other anti-apoptotic genes such as *BCL2* and *MCL1*.[26–28] These findings suggest that tumors resistant to radiation may exhibit cancer stem cell-like features. Several studies have shown that cancer stem cell-like cells may promote a pro-inflammatory microenvironment by constitutive NF-κB activity and cytokine and chemokine production.[29–32] However, such data are not available in SCLC.

Recently, a new Bcl2Bcl-XL inhibitor, ABT-737, has demonstrated some efficacy in SCLC and CLL cells through induction of apoptosis.[33,34] Phase I/II clinical trials are assessing the safety and utility of navitoclax, an ABT-737 derivative that can be administered orally, on SCLC and CLL.[17,18] A platelet-sparing potent BCL-2-selective inhibitor ABT-199 has recently been developed[35] and was recently shown to elicit promising tumor responses in BCL-2-dependent hematopoietic malignancies.[36] Some studies have shown a benefit from combining chemotherapy and ABT-737, so far, the molecular bases of this interaction are not well-known although it has been hypothesized that induction of Noxa by CPT-11 in colorectal carcinoma[37,38] or Mcl-1 downregulation by various chemotherapy regimens[38,39] may explain positive interaction. One study demonstrated that combining ABT-737 and carboplatinum resulted in an enhancement of chemotherapy efficacy in a sequence-dependence manner.[39] Only the sequence of administration in which carboplatin was followed by that of ABT-737 revealed synergistic interactions in ovarian cancer both *in vitro* and *in vivo*. In our study, we showed that using S44563 during fractionated irradiation increases the efficacy of radiation and that this effect was greater when S44563 was given after the completion of the radiation in SCLC. These data are consistent with a model in which radiation sensitizes tumor cells ready for apoptosis induction by S44563 because the upregulation of S44563 targets Bcl-2 and Bcl-X$_L$. Previous studies described that Mcl-1 and Bcl2A1 expression was associated with primary and secondary resistance to Bcl-2/Bcl-X$_L$ inhibitors,[40–44] a finding that was confirmed in our study. These proteins are not inhibited by current BH3 mimetics including S44563 and may result in resistance and relapse to the triple combination.

We also investigated the value of the combination of S44563 with cisplatin-based chemo-radiotherapy. Most preclinical studies assessing the association between a new drug and radiation are performed out of the context of standard care. Epidermal growth factor receptor in combination with radiation using the C225 antibody was effective in terms of local control and survival.[45,46] However, cisplatin-based radiochemotherapy represents the standard approach for advanced head and neck cancer. The combination of radiation, cisplatin and C225 has been tested clinically before a thorough preclinical evaluation of the combined therapy. The results of a phase 3 trial assessing the triple combination did not show any benefit from the addition of cetuximab to cisplatin in combination with radiation.[47] Recently, guidelines for preclinical and early phase clinical assessment of novel radiosensitizers recommended to design preclinical experiments including standard treatment such as the combination of radiation and chemotherapy.[48] Here, we demonstrated that S44563 enhanced the efficacy of the standard cisplatin-based chemo-radiotherapy used to treat localized SCLC. Indeed, some mice cured exhibited long-lasting complete responses with a follow-up greater than 260 days. Of note, we did not observe any signs of severe lung damage such as endothelial damage and fibrosis-like lesions that would have been exacerbated by S44563. These data suggested that S44563 has no major toxic effects on normal lung tissue, even in the context of IR.

In summary, pharmacological inhibition of Bcl-2 and Bcl-X$_L$ proteins could restore sensitivity to radiation in a model of SCLC both *in vitro* and *in vivo*. Radiation-induced overexpression of anti-apoptotic proteins made SCLC susceptible to apoptosis induction by S44563. S44563 synergized with cisplatin-based chemoradiotherapy and did not cause any significant lung toxicity. Altogether, these results prepare the bases for the design of future clinical trials in SCLC patients.

Materials and Methods

Reagent. S44563 (dihydrochloride) has a molecular weight of 912.4 (839.479 + 72.922) and its molecular formula is $C_{44}H_{47}ClN_6O_5S_2$, 2 HCl. It has two asymmetric carbons. The purity of the batches ranges between 97.8 and 99.9% and the optical purity was 99%. S44563-2 was synthesized at Institut de Recherches Servier, the synthesis will be published elsewhere (initial patent application filed in France 02/02/2007 under N 07/00741) (Figure 1a). *P65* siRNA (Santa Cruz, Santa Cruz, CA, USA; sc-29410, final concentration: 15 nmol/l) was transfected into cells using Amaxa *Nucleofector* Technology (Lonza Inc, Levallois-Perret, France) according to the manufacturer's recommendations.

Cells and culture conditions. Human SCLC cell lines, H146, H69 and H196 were purchased from ATCC (Manassas, VA, USA). These cells were maintained in RPMI 1640 supplemented with 2 mM L-glutamine, 10% fetal bovine serum (Gibco, Cergy-Pontoise, France), 100 units/ml of penicillin and 10 000 μg/ml of streptomycin. MV4-11, RS4;11 and HCT116 cell lines were purchased from ATCC. All cells were incubated at 37 °C in a humidified atmosphere of 5% CO_2 in air.

X-ray irradiation. Cells were irradiated at room temperature using a 200-kV X-ray irradiator at a dose rate of 0.85 Gy/min. For *in vivo* irradiation, radiation was given using mouse jigs designed to expose only the tumor bed to radiation at a dose rate of 1.1 Gy/min.

Fluorescence polarization assays. A fluorescent BH3 peptide (BH3 motif from the protein Puma) was incubated with either recombinant Bcl-2 or Bcl-X$_L$ protein (20 mM Na_2HPO_4 pH 7.4, 50 mM NaCl, 1 mM EDTA, 0.05% pluronic acid). Upon binding, the fluorescence emitted by the BH3 peptide becomes polarized. The inhibition of the interaction between the fluorescent BH3 peptide and Bcl-2 or Bcl-X$_L$ is followed by measuring a decrease in fluorescence polarization. In these assays, Bcl-2 or Bcl- X$_L$ concentration was 100 nM, the fluorescent BH3 peptide concentration was 15 nM and S44563 was titrated from 1 nM to 100 μM.

DEVDase assay. H146 SCLC cells were exposed to increasing concentrations of S44563 for 6 h and DEVDase activity (Promega, Lyon, France) was measured in cell extracts prepared in lysis buffer.

Co-immunoprecipitation assays. H146 cells were exposed to increasing concentrations of S44563-2 for 2 h and cell lysates were prepared in immunoprecipitation buffer (Hepes 10 mM pH 7.5, KCl 150142 mM, $MgCl_2$ 5 mM, EDTA 1 mM, Triton 0.4%) supplemented with protease inhibitors.

Cell lysates were then subjected to an immunoprecipitation with an anti-Bcl-2 antibody (sc-509). The presence of Bax in the anti-Bcl-2 immunoprecipitate (IPs) and lysates was then evaluated by immunoblot analysis using an anti-Bax antibody (Santa Cruz, sc-493).

Measurement of cell growth. Cells were seeded in 96-well plates, 24 h before incubation with various concentrations of S44563 for 72 h. The number of viable cells was determined by using WST-1 assay according to the manufacturer's instructions (Roche, Meylan, France).

Clonogenic survival. Clonogenic assays were performed without irradiation and with various doses of S44563 to assess dose response and calculate the concentration of S44563 to inhibit 50% of cells (IC_{50}). After exposure with S44563 at doses ranging from 100 nmol/l to 10 μmol/l for 12 h, cells were exposed to radiation at doses ranging from 2 to 6 Gy using 200 kV X-rays; they were then separated, counted and seeded for colony formation in 35-mm dishes at 500–10 000 cells/dish. Upon incubation intervals of 21–28 days, colonies were stained with crystal violet and manually counted. All colonies of 50 cells or more were then counted. For floating cells (H146 and H69), the cells were incubated in methylcellulose-based medium as described previously.[49] The SF was estimated according to the formula: SF = number of colonies formed/number of cells seeded plating efficiency of the control group. The radiation dose enhancement ratio (DER) by S44563 was calculated using the following formula: DER = (SF at an indicated dose of radiation alone)/(SF at an indicated dose of radiation + S44563). DER = 1 suggests an additive radiation effect and DER > 1, a supra-additive effect as against a sub-additive effect in the case of DER < 1.

Cytofluorometric analysis. Cells were stained with the following probes to assess apoptosis-associated modifications: propidium iodide (final concentration of 2 μg/ml, Sigma-Aldrich, Lyon, France) for viability and dihexyloxacarbocyanine iodide ($DiOC_6(3)$, 40 nmol/l, Molecular Probes, Saint-Aubin, France) for $\Delta\psi_m$ dissipation (after overnight fixation of the cells in glacial 70% ethanol, DNA content was quantified by staining with propidium iodide (20 μg/ml), RNase (100 μg/ml, Sigma) and EDTA (20 mmol/l) for 30 min at room temperature.[50] Stained nuclei were analyzed for DNA-propidium iodide fluorescence using a Becton Dickinson (Rungis, France) FACSCaliburs flow cytometer.

Microarrays studies and multiplex PCR. For transcriptome analysis, 10^6 cells were seeded in T25 flasks, allowed to grow for 24 h and then left untreated or treated with 2 Gy radiation. After 24 h, cells were harvested, lysed for the extraction of RNA and processed to analyze gene expression, as previously reported.[50] Raw data have been submitted to ArrayExpress (accession numer: E-MTAB-966). For PCR analysis, 10^6 cells were seeded in T25 flasks, allowed to grow for 24 h and then left untreated or treated 6 Gy radiation and harvested either 2 or 24 h after the treatment. *Apoptosis* TaqMan Low Density Array (TLDA) custom-designed format from Applied-Biosystems (Villebon-sur-Yvette, France) were used as duplicates for each gene expression per sample using the Applied Biosystems 7900HT Real-Time PCR system. The results of each plate were analyzed using ABI PRISM software to calculate the C_T value of each well and compare these values in studied gene wells with endogenous control wells.

Analysis of protein expression. Protein samples of SCLC cells were prepared in lysis buffer, according to standard established protocols.[49] Extracted proteins were separated by 12% SDS-PAGE and subjected to immunoblots using mouse monoclonal IgG1 antibodies specific for active caspase-8 (Cell Signalling Technology, Leiden, Netherlands), or glyceraldehyde-3-phosphate dehydrogenase (GAPDH; Millipore, Guyancourt, France) and rabbit polyclonal antibodies against caspase-3, active caspase-9 (Cell Signalling Technology). To fractionate cytoplasmic and nuclear proteins, cells were washed and incubated on ice for 10 min in buffer A (10 mM HEPES pH 7.9, 10 mM KCl, 0.1 mM EDTA, 0.5% NP-40, 1 mM phenylmethylsulfonyl fluoride and a cocktail of protease inhibitor). Supernatants containing the cytoplasmic extracts were separated by centrifugation (10 000 *g*, 5 min). Pellets were suspended in buffer B (20 mM HEPES pH 7.9, 400 mM KCl, 1 mM EDTA, 10% glycerol, 1 mM phenylmethylsulfonyl fluoride and a cocktail of protease inhibitors) and incubated at 4 °C for 1 h with mixing. The resulting nuclear lysates were clarified with high-speed centrifugation. RELA/p65 antibody was obtained from BD Biosciences (Le Pont de Claix, France) (1 : 500).

A tissue array that includes localized SCLC samples at diagnosis from the 29 patients was constructed at the Department of Pathology, Institut Gustave Roussy. Immunostainings were carried out for Bcl-2 (clone 124, Dako Cytomation, Les Ulis, France; 1 : 25 dilution), Bcl-X_L (Ab-2, clone 7D9; Lab Vision, Thermo scientific, Villebon-sur-Yvette, France; 1 : 150 dilution), Mcl-1 (clone ab28147, Abcam, Paris, France; 1 : 50 dilution). Bcl-2, Bcl-X_L and Mcl-1 expressions were evaluated by a composite score that consisted in the product of intensity and percentage of tumor cells stained.

Assay for tumor growth in immunocompromised mice. The *in vivo* experiments were carried out at the Institut Gustave Roussy under the Animal Care license n°C94-076-11 (French Ministry of Agriculture). Female athymic nude or nod/scid mice (6–8-weeks old) obtained from Janvier CERT (Le Genest St. Isle, France) were used. H146 and H69 cells were harvested in exponential phase growth and 5×10^6 cells were injected subcutaneously into the flank area of 6–8-week-old female mice on day 0. H196 cells were not used for *in vivo* studies as we are unable to obtain H196 xenografts in nude or SCID mice.

For antitumor activity in the SCLC H146 model, S44563 was administered daily in 1% Tween80/water for 21 days at two doses: 100 and 150 mg/kg by the intra peritoneal (i.p.) route.

For combination studies, mice were randomized into 6–10 mice per group when tumors reached appropriate size and treated with S44563 or saline solution 100 mg/kg i.p q.d $\times 5$, $\times$ 1 week, or irradiation with 2 Gy/day for 4 days or the combination of S44563-2 and irradiation. When cisplatin was administered, the dose was 1 mg/kg daily given twice per week for 2 weeks. Mice were weighed, and the tumor size was measured twice a week. The tumor volume was estimated from two-dimensional tumor measurements by the formula:

$$\text{Tumor volume} = \text{length}(\text{mm}) \times \text{width}^2(\text{mm}^2)/2.$$

In each group, the relative tumor volume was expressed as the *Vt*/*Vo* ratio (*Vt* is the mean tumor volume on a given day during the treatment and *Vo* is the mean tumor volume at the beginning of the treatment). The absolute growth delay was calculated to compare the efficacy of each regimen. Absolute growth delay is defined as the time in days for tumors in the treatment arm to triple their initial volume (RTV3) minus the time in days for tumors untreated to reach RTV3. Dose enhancement factor (DEF) by S44563 was calculated using the following formula: DEF = (Absolute growth delay in combination group)/(Absolute growth delay in radiation group).

Assessment of lung toxicity. The potential fibrotic effects triggered by S44563 and the combination of S44563 with radiation were assessed in the well-characterized model of bleomycin (BLM)-induced lung fibrosis.[51] Intra-peritoneal injection of BLM (40 mg/kg) was performed for 5 days. Fibrosis occurrence was monitored 4 weeks after initiation of BLM administration. Nude mice were divided in six groups: control, BLM, IR (19 Gy), S44563, BLM-S44563 and IR-S44563. At week 4, the lungs from control, BLM (positive control), S44563 and S44563-BLM groups were collected for histology and were fixed in Finefix (Milestone Medical, Sorisole, Italy) and paraffin embedded. At week 15, the lungs from control, S44563, IR and IR-S44563 groups were collected as others groups. Sections were stained with Hematoxylin-Eosin-Safranin and examined using conventional light microscopy. Tissue lesions were scored as fibrotic in each of the subpleural, vascular and intraparenchymal areas. Inflammatory infiltrates were also scored by the same pathologist (PO).

Statistical analysis. Statistic significance was evaluated using two-tailed Student *t* tests or ANOVA. When ANOVA was significant, pairwise comparisons using permutational *t*-tests using false discovery rate correction were used. *P* values < 0.05 were considered statistically significant. For *in vivo* studies, two-way ANOVA was used with R software for statistical comparisons involving multiple groups to determine the significance of each of two groups ($P < 0.05$). Paired or unpaired two-tailed Student's *t* test was used in comparisons between two groups. Survival was determined using Kaplan–Meier method and compared using log-rank tests.

Conflict of Interest

Eric Deutsch's work has been funded by Servier, Inc. Olivier Geneste Alain Pierre, Laurence Kraus Berthier and Stephane Depil are employees of Servier. The remaining authors declare no conflict of interest.

Acknowledgements. GK is supported by the Ligue Nationale contre le Cancer (Equipes labellisée), Agence Nationale pour la Recherche, European Commission (ChemoRes), Fondation pour la Recherche Médicale (FRM), Institut National du Cancer (INCa), Fondation de France, Cancéropôle Ile-de-France, Fondation Bettencourt-Schueller and the LabEx Immuno-Oncology. ED is supported by the Assocciation pour la Recherche contre le Cancer (ARC), Electricité de France (EDF), Cancéropôle Ile-de France. This manuscript has been supported by Institut de Recherche Servier.

1. Hanahan D, Weinberg RA. Hallmarks of cancer: the next generation. *Cell* 2011; **144**: 646–674.
2. Adams JM, Cory S. The Bcl-2 apoptotic switch in cancer development and therapy. *Oncogene* 2007; **26**: 1324–1337.
3. Strasser A, Harris AW, Jacks T, Cory S. DNA damage can induce apoptosis in proliferating lymphoid cells via p53-independent mechanisms inhibitable by Bcl-2. *Cell* 1994; **79**: 329–339.
4. Rupnow BA, Murtha AD, Alarcon RM, Giaccia AJ, Knox SJ. Direct evidence that apoptosis enhances tumor responses to fractionated radiotherapy. *Cancer Res* 1998; **58**: 1779–1784.
5. Amundson SA, Myers TG, Scudiero D, Kitada S, Reed JC, Fornace AJ. An informatics approach identifying markers of chemosensitivity in human cancer cell lines. *Cancer Res* 2000; **60**: 6101–6110.
6. Wacheck V, Selzer E, Gunsberg P, Lucas T, Meyer H, Thallinger C *et al.* 2003Bcl-XL antisense oligonucleotides radiosensitise colon cancer cells. *Br J Cancer* **89**: 1352–1357.
7. Levi F, Lucchini F, Negri E, Boyle P, La Vecchia C. Mortality from major cancer sites in the European Union, 1955-1998. *Ann Oncol* 2003; **14**: 490–495.
8. Govindan R, Page N, Morgensztern D, Read W, Tierney R, Vlahiotis A *et al.* Changing epidemiology of small-cell lung cancer in the United States over the last 30 years: analysis of the surveillance, epidemiologic, and end results database. *J Clin Oncol* 2006; **24**: 4539–4544.
9. Spira A, Ettinger DS. Multidisciplinary management of lung cancer. *N Engl J Med* 2004; **350**: 379–392.
10. Lally BE, Geiger AM, Urbanic JJ, Butler JM, Wentworth S, Perry MC *et al.* Trends in the outcomes for patients with limited stage small cell lung cancer: An analysis of the Surveillance, Epidemiology, and End Results database. *Lung Cancer* 2009; **64**: 226–231.
11. Kim YH, Girard L, Giacomini CP, Wang P, Hernandez-Boussard T, Tibshirani R *et al.* Combined microarray analysis of small cell lung cancer reveals altered apoptotic balance and distinct expression signatures of MYC family gene amplification. *Oncogene* 2006; **25**: 130–138.
12. Brambilla E, Negoescu A, Gazzeri S, Lantuejoul S, Moro D, Brambilla C *et al.* Apoptosis-related factors p53, Bcl2, and Bax in neuroendocrine lung tumors. *Am J Pathol* 1996; **149**: 1941–1952.
13. Sartorius UA, Krammer PH. Upregulation of Bcl-2 is involved in the mediation of chemotherapy resistance in human small cell lung cancer cell lines. *Int J Cancer* 2002; **97**: 584–592.
14. Jonathan EC, Bernhard EJ, McKenna WG. How does radiation kill cells? *Curr Opin Chem Biol* 1999; **3**: 77–83.
15. Sirzén F, Zhivotovsky B, Nilsson A, Bergh J, Lewensohn R. Spontaneous and radiation-induced apoptosis in lung carcinoma cells with different intrinsic radiosensitivities. *Anticancer Res* 1998; **18**: 695–699.
16. Butterfield L, Storey B, Maas L, Heasley LE. c-Jun NH2-terminal kinase regulation of the apoptotic response of small cell lung cancer cells to ultraviolet radiation. *J Biol Chem* 1997; **272**: 10110–10116.
17. Gandhi L, Camidge DR, Ribeiro de Oliveira M, Bonomi P, Gandara D, Khaira D *et al.* Phase I Study of Navitoclax (ABT-263), a Novel Bcl-2 Family Inhibitor, in Patients With Small-Cell Lung Cancer and Other Solid Tumors. *J Clin Oncol* 2011; **29**: 909–916.
18. Wilson WH, O'Connor OA, Czuczman MS, LaCasce AS, Gerecitano JF, Leonard JP *et al.* Navitoclax, a targeted high-affinity inhibitor of BCL-2, in lymphoid malignancies: a phase 1 dose-escalation study of safety, pharmacokinetics, pharmacodynamics, and antitumour-antitumor activity. *Lancet Oncol* 2010; **11**: 1149–1159.
19. Beroukhim R, Mermel CH, Porter D, Wei G, Raychaudhuri S, Donovan J *et al.* The landscape of somatic copy-number alteration across human cancers. *Nature* 2010; **18**: 899–905.
20. Tahir SK, Yang X, Anderson MG, Morgan-Lappe SE, Sarthy AV, Chen J *et al.* Influence of Bcl-2 family members on the cellular response of small-cell lung cancer cell lines to ABT-737. *Cancer Res* 2007; **67**: 1176–1183.
21. Oltersdorf T, Elmore SW, Shoemaker AR, Armstrong RC, Augeri DJ, Belli BA *et al.* An inhibitor of Bcl-2 family proteins induces regression of solid tumours. *Nature* 2005; **435**: 677–681.
22. Olejniczak ET, Van Sant C, Anderson MG, Wang G, Tahir SK, Sauter G *et al.* Integrative genomic analysis of small-cell lung carcinoma reveals correlates of sensitivity to bcl-2 antagonists and uncovers novel chromosomal gains. *Mol Cancer Res* 2007; **5**: 331–339.
23. Chen A, Edelstein LC, Gélinas C. The Rel/NF-κB Family Directly Activates Expression of the Apoptosis Inhibitor Bcl-xL. *Mol Cell Biol* 2000; **20**: 2687–2695.
24. Jinawath N, Vasoontara C, Jinawath A, Fang X, Zhao K, Yap KL *et al.* Oncoproteomic analysis reveals co-upregulation of RELA and STAT5 in carboplatin resistant ovarian carcinoma. *PLoS One* 2010; **5**: e11198.
25. Park D, Magis AT, Li R, Owonikoko TK, Sica GL, Sun SY *et al.* Novel small-molecule inhibitors of Bcl-XL to treat lung cancer. *Cancer Res* 2013; **73**: 5485–5496.
26. Begg AC, Stewart FA, Vens C. Strategies to improve radiotherapy with targeted drugs. *Nat Rev Cancer* 2011; **11**: 239–253.
27. Karin M. Nuclear factor-kappaB in cancer development and progression. *Nature* 2006; **441**: 431–436.
28. De Bacco F, Luraghi P, Medico E, Reato G, Girolami F, Perera T *et al.* Induction of MET by ionizing radiation and its role in radioresistance and invasive growth of cancer. *J Natl Cancer Inst* 2011; **103**: 645–661.
29. Alvero AB, Chen R, Fu HH, Montagna M, Schwartz PE, Rutherford T *et al.* Molecular phenotyping of human ovarian cancer stem cells unravels the mechanisms for repair and chemoresistance. *Cell Cycle* 2009; **8**: 158–166.
30. Liu M, Sakamaki T, Casimiro MC, Willmarth NE, Quong AA, Ju X *et al.* The canonical NF-kappaB pathway governs mammary tumorigenesis in transgenic mice and tumor stem cell expansion. *Cancer Res* 2010; **70**: 10464–10473.
31. Vilimas T, Mascarenhas J, Palomero T, Mandal M, Buonamici S, Meng F *et al.* Targeting the NF-kappaB signaling pathway in Notch1-induced T-cell leukemia. *Nat Med* 2007; **13**: 70–77.
32. Yip NC, Fombon IS, Liu P, Brown S, Kannappan V, Armesilla AL *et al.* Disulfiram modulated ROS-MAPK and NFκB pathways and targeted breast cancer cells with cancer stem cell-like properties. *Br J Cancer* 2011; **104**: 1564–1574.
33. Hann CL, Daniel VC, Sugar EA, Dobromilskaya I, Murphy SC, Cope L *et al.* Therapeutic efficacy of ABT-737, a selective inhibitor of BCL-2, in small cell lung cancer. *Cancer Res* 2008; **68**: 2321–2328.
34. Del Gaizo Moore V, Brown JR, Certo M, Love TM, Novina CD, Letai A. Chronic lymphocytic leukemia requires BCL2 to sequester prodeath BIM, explaining sensitivity to BCL2 antagonist ABT-737. *J Clin Invest* 2007; **117**: 112–121.
35. Souers AJ, Leverson JD, Boghaert ER, Ackler SL, Catron ND, Chen J *et al.* ABT-199, a potent and selective BCL-2 inhibitor, achieves antitumor activity while sparing platelets. *Nat Med* 2013; **19**: 202–208.
36. Vandenberg CJ, Cory S. ABT-199, a new Bcl-2-specific BH3 mimetic, has in vivo efficacy against aggressive Myc-driven mouse lymphomas without provoking thrombocytopenia. *Blood* 2013; **121**: 2285–2288.
37. Okumura K, Huang S, Sinicrope FA. Induction of Noxa sensitizes human colorectal cancer cells expressing Mcl-1 to the small-molecule Bcl-2/Bcl-xL inhibitor, ABT-737. *Clin Cancer Res* 2008; **14**: 8132–8142.
38. Olberding KE, Wang X, Zhu Y, Pan J, Rai SN, Li C. Actinomycin D synergistically enhances the efficacy of the BH3 mimetic ABT-737 by downregulating Mcl-1 expression. *Cancer Biol Ther* 2010; **10**: 918–929.
39. Witham J, Valenti MR, De-Haven-Brandon AK, Vidot S, Eccles SA, Kaye SB *et al.* The Bcl-2/Bcl-XL family inhibitor ABT-737 sensitizes ovarian cancer cells to carboplatin. *Clin Cancer Res* 2007; **13**: 7191–7198.
40. Touzeau C, Dousset C, Linda B, Gomez-Bougie P, Bonnaud S, Moreau A *et al.* ABT-737 induces apoptosis in mantle cell lymphoma cells with a Bcl-2high/Mcl-1low profile and synergizes with other anti-neoplastic agents. *Clin Cancer Res* 2011; **17**: 5973–5981.
41. Yecies D, Carlson NE, Deng J, Letai A. Acquired resistance to ABT-737 in lymphoma cells that up-regulate MCL-1 and BFL-1. *Blood* 2010; **115**: 3304–3313.
42. Lestini BJ, Goldsmith KC, Fluchel MN, Liu X, Chen NL, Goyal B *et al.* Mcl1 downregulation sensitizes neuroblastoma to cytotoxic chemotherapy and small molecule Bcl2-family antagonists. *Cancer Biol Ther* 2009; **8**: 1587–1595.
43. Vogler M, Butterworth M, Majid A, Walewska RJ, Sun XM, Dyer MJ *et al.* Concurrent up-regulation of BCL-XL and BCL2A1 induces approximately 1000-fold resistance to ABT-737 in chronic lymphocytic leukemia. *Blood* 2009; **113**: 4403–4413.
44. Al-Harbi S, Hill BT, Mazumder S, Singh K, Devecchio J, Choudhary G *et al.* An anti-apoptotic Bcl-2 family expression index predicts the response of chronic lymphocytic leukemia to ABT-737. *Blood* 2011; **118**: 3579–3590.
45. Krause M, Schutze C, Petersen C, Pimentel N, Hessel F, Harstrick A *et al.* Different classes of EGFR inhibitors may have different potential to improve local tumourtumor control after fractionated irradiation: a study on C225 in FaDu hSCC. *Radiother Oncol* 2005; **74**: 109–115.
46. Bonner JA, Harari PM, Giralt J, Azarnia N, Shin DM, Cohen RB *et al.* Radiotherapy plus cetuximab for squamous-cell carcinoma of the head and neck. *N Engl J Med* 2006; **354**: 567–578.
47. Ang KK, Zhang QE, Rosenthal DI, Nguyen-Tan P, Sherman EJ, Weber RS *et al.* A randomized phase III trial (RTOG 0522) of concurrent accelerated radiation plus cisplatin with or without cetuximab for stage III-IV head and neck squamous cell carcinomas (HNC). *J Clin Oncol* 2011; **29**: (suppl; abstr 5500).
48. Harrington KJ, Billingham LJ, Brunner TB, Burnet NG, Chan CS, Hoskin P *et al.* NCRI Clinical and Translational Radiotherapy Research Working Group Guidelines for preclinical

and early phase clinical assessment of novel radiosensitisers. *Br J Cancer* 2011; **105**: 628–639.

49. Loriot Y, Mordant P, Brown BD, Bourhis J, Soria JC, Deutsch E. Inhibition of BCL-2 in small cell lung cancer cell lines with oblimersen, an antisense BCL-2 oligodeoxynucleotide (ODN): in vitro and in vivo enhancement of radiation response. *Anticancer Res* 2010; **30**: 3869–3878.
50. de La Motte Rouge T, Galluzzi L, Olaussen KA, Zermati Y, Tasdemir E, Robert T *et al.* A novel epidermal growth factor receptor inhibitor promotes apoptosis in non-small cell lung cancer cells resistant to erlotinib. *Cancer Res* 2007; **67**: 6253–6262.
51. Monceau V, Pasinetti N, Schupp C, Pouzoulet F, Opolon P, Vozenin MC. Modulation of the Rho/ROCK pathway in heart and lung after thorax irradiation reveals targets to improve normal tissue toxicity. *Curr Drug Targets* 2010; **11**: 1395–1404.

Supplementary Information accompanies this paper on Cell Death and Disease website (http://www.nature.com/cddis)